Codeposition of Amorphous Nickel-Chromium (Nichrome) Thin Film Alloys from Complexing Cr(III) Formate-Glycine Baths

Magdy A.M. Ibrahim,[1,2] S.N. Alamri[1] and M. Emad[1]*

[1]*Chemistry Department, Faculty of Science, Taibah University, Al Madinah Al Mounwara, Kingdom of Saudi Arabia*
[2]*Chemistry Department, Faculty of Science, Ain Shams University, Abbassia, Cairo, Egypt*

Amorphous Ni-Cr thin film alloys were produced successfully on steel substrates from complexing Cr(III) formate-glycine baths (pH 7.0) by electrodeposition. The deposition was carried out galvanostatically under different conditions of concentrations of electrolyte, current density and bath temperature. It was found that the chromium content in the alloy was in the range of 1.5 - 28 at% depending on the operating conditions. The chromium content in the deposit increased with an increase in Ni(II) ion content as well as with Cr(III) ion content. However, the chromium decreased with increasing bath temperature. Cyclic voltammetry and potentiodynamic polarization measurements showed that the Ni-Cr deposition potential lies at a more noble potential than those of the parent metals indicating that chromium forms a solid solution with nickel. The chronoamperometric measurements indicate that the initial growth of Ni-Cr film codeposition is a diffusion-controlled process. The XRD measurements showed that all Ni-Cr alloy deposits were amorphous.

Keywords: *Ni-Cr alloy, electrodeposition, cyclic voltammetry, polarization, chronoamperometry.*

Introduction

Chromium alloy deposits have found use in several industrial applications because they exhibit considerable resistance to wear, abrasion and hardness as well as corrosion.[1] In addition, chromium is used extensively as a decorative coating together with nickel as an undercoat in metal finishing industries.[2] It is found that, the introduction of small amounts (< 7%) of chromium to nickel, increases the sensitivity of the alloy to oxidation and a marked increase in electrical resistivity is observed with increasing chromium content. An additional level of 20% chromium is considered the optimum for electrical resistance wires suitable for heating elements. Moreover, Ni-Cr casting alloys can be used in dental crown and bridge applications.[3] Recently, the electrodeposition technique was used to prepare Ni-Cr alloy foams.[4]

Conventional chromium coatings electrodeposited from Cr(VI) solutions have been used for more than 100 years. However, environmental considerations have been responsible for increased interest in less toxic trivalent chromium electrodeposition baths as an alternative to the conventional highly toxic hexavalent chromium baths.[5,6] Therefore, many attempts have been made over the last decades to deposit coatings of chromium alloys from Cr(III) electrolytes.[7,8] It is almost impossible to deposit a chromium coating from a simple aqueous Cr(III) solution due to the very stable $[Cr(H_2O)_6]^{+3}$ complex. For this reason, destabilization of this complex should take place by using suitable ligands. Therefore, complexing agents play a significant role in the plating bath solution in producing good quality coatings[9] and the selection of suitable complexing agents is essential.

Continuing our work on the electrodeposition of metals and alloys[8-14] from environmentally friendly electrolytes, the present work was undertaken to develop a Cr(III) electrolyte containing glycine and ammonium formate as complexing agents from which Ni-Cr alloys could be codeposited. Cr(III) electrolytes are particularly attractive because they do not pollute the environment and are non-toxic. In addition, the study aimed to investigate the factors influencing chromium content, morphology, alloy composition and alloy current efficiency.

* *Corresponding author:*
Dr. Magdy A.M. Ibrahim
Chemistry Department
Faculty of Science
Ain Shams University
Abbassia, Cairo, Egypt.
Phone: 966501221667
Fax: 966048470235
E-mail: imagdy1963@hotmail.com

Experimental procedure

Codeposition was carried out at room temperature (25°C) under galvanostatic conditions. For deposition, 2.5 × 3.0 cm steel sheets were used as cathodes. A 2.5 × 3.0 cm platinum sheet was used as an anode. The plating cell was a rectangular Perspex trough (10 × 3 cm) provided with vertical grooves, on each of the side walls, to fix the electrodes. Before each run, the steel cathode was mechanically polished with different grades of emery papers (600, 800, 1000 and 1500 grit) then washed with distilled water, rinsed with ethanol and weighed. Direct current was supplied by a DC power supply unit.

The percentage cathodic current efficiency (CCE%) of the alloy deposition was determined from the mass and composition of the deposited alloy and the charged passed[15] Deposition was carried out for 15 minutes in each case. The electrodeposition was carried out without separating membranes.

Potentiodynamic cathodic polarization curves were recorded using steel substrates by sweeping the potential from the rest potential in the negative direction at scan rate of 20 mV/sec. A Solartron SI 1287 computer-controlled potentiostat /galvanostat was used for all the electrochemical measurements. The classic three-electrode cell was used for the cyclic voltammetry (CV) measurements at scan rate of 50 mV/sec. The working electrode was a glassy carbon rod (area 0.1963 cm^2) embedded in a PVC cylinder. The glassy carbon electrode (GCE) was polished before each run with diamond paste (0.25 μm) until a mirror surface was obtained, then washed several times with doubly distilled water. The counter electrode was a platinum wire. All potentials were measured relative to a saturated calomel electrode (SCE). To avoid contamination, the reference electrode was connected to the working cathode via a salt bridge provided with a Luggin-Haber tip and filled with the solution under test.

The corrosion behavior of some samples coated with Ni-Cr thin film on steel was investigated in 0.1M NaOH solution using a three-electrode system with a platinum counter electrode and a saturated calomel reference electrode. The corrosion current densities (i_{corr}) were determined from Tafel extrapolation. To begin the measurements, the sample was introduced into the cell immediately after electrodeposition and was allowed to reach equilibrium. Polarization measurements were performed under potentiodynamic conditions with a potential scan rate of 10 mV/sec. In all cases, duplicate experiments were carried out to ensure reproducibility.

The composition of the codeposited Ni-Cr alloy and the surface morphology of the as-deposited Ni-Cr film were determined using energy dispersive x-ray spectroscopy (EDS) combined with Shimadzu Super-scan SSX-550 scanning electron microscope, respectively. The crystalline structure of the Ni-Cr alloy deposited on steel was examined by x-ray diffraction (Shimadzu XRD-6000) using a diffractometer (40 kV, 20 mA) with a Ni filter and Cu Kα radiation.

Results and discussion

Preliminary experiments were conducted to achieve a suitable bath composition for producing fine, bright, compact and highly adherent coatings of Ni-Cr thin film alloy. The suitable bath composition found to produce good quality coatings of Ni-Cr alloy is given in Table 1. The advantage of this bath is its ability to produce Ni-Cr films with very good adhesion and appearance without addition agents. Moreover, the presence of formate and glycine do not completely stop but only delay the process of formation of the stable and inert oligomeric species and thus provide a prolonged working lifetime of Cr(III) formate-glycine bath.

Evidence in the literature[16-18] has suggested that the electrodeposition of chromium from simple trivalent baths involves two consecutive reduction steps of Cr^{+3} species to $Cr_{(s)}$:

$$Cr^{+3} + e^- \rightarrow Cr^{+2} \qquad E_0 = -0.41\ V_{SHE} \qquad (1)$$

$$Cr^{+2} + 2e^- \rightarrow Cr_{(s)} \qquad E_0 = -0.91\ V_{SHE} \qquad (2)$$

where E_0 is the standard electrode potential at 25°C. Combining Equations (1) and (2) gives the overall reduction reaction of Cr^{+3} ions to $Cr_{(s)}$:

$$Cr^{+3} + 3e^- \rightarrow Cr_{(s)} \qquad E_0 = -0.74\ V_{SHE} \qquad (3)$$

In addition, in aqueous trivalent chromium solution, hydrogen gas evolution is the most dominant reduction reaction during the chromium plating process. Therefore, hydrogen evolution reaction occurs simultaneously at the cathode:

$$2H_2O + 2e^- \rightarrow H_{2(g)} + 2OH^- \qquad E_0 = -0.12\ V_{SHE} \qquad (4)$$

Chemistry of Cr(III) with formate and glycine

Glycine is an amino acid usually presented as $H_2N\text{-}CH_2\text{-}COOH$ (Gly). In aqueous solutions many forms are found depending on the solution pH, as shown by the following equations:

$$^+H_3N\text{-}CH_2\text{-}COOH \leftrightarrow {}^+H_3N\text{-}CH_2\text{-}COO^- + H^+, \quad pK_a = 2.47 \qquad (5)$$

$$^+H_3N\text{-}CH_2\text{-}COO^- \leftrightarrow H_2N\text{-}CH_2\text{-}COO^- + H^+, \quad pK_a = 9.66 \qquad (6)$$

As it can be seen, depending on the solution pH, glycine exists as a cation in acid solution, a charge neutral zwitterion at intermediate pH values, or an anion in basic media. Consequently, metal complexes formed with glycine depend strongly on the pH of the solution.

In aqueous solutions, Cr(III) ions exist in various complex forms[19], such as $[Cr(H_2O)_6]^{+3}$, $[(H_2O)_4Cr(OH)(OH)Cr(H_2O)]^{+4}$, $[(H_2O)_5Cr(OH)Cr(H_2O)_5]^{+5}$, $[Cr(H_2O)_5(OH)]^{+2}$, $[Cr(H_2O)_5Cl]^{+2}$, etc.

However, when formate or glycine are present, one or more of the H_2O, Cl^- or OH^- species of the inorganic Cr(III) complexes may be replaced by the organic ligand to form organo-chromium complexes such as $[Cr(H_2O)_5(HCOO)]^{+2}$ and $[Cr(H_2O)_4(Gly)]^{+2}$.

The formation of such complexes species decreases the concentration of the electroactive free chromium species. As the Cr(III) glycine-formate complexes are formed, it would be expected that the complex formation might affect the electrochemical reduction behavior of Cr(III) in the bath, therefore, codeposition of nickel and chromium can be realized by complex formation.

In the absence of formate and glycine in the plating bath, no chromium electrodeposition could be observed and only nickel deposition could be detected. This suggests that the following reduction steps are possible in the absence of formate and glycine:

$$[Cr(H_2O)_5Cl]^{+2} + e^- = [Cr(H_2O)_5]^{+2} + Cl^- \qquad (7)$$

The $[Cr(H_2O)_5]^{+2}$ complex in Equation (7) is very inert and stable and cannot be further reduced at the cathode.

Table 1

Composition of the electroplating solutions

Bath Number	Concentration						
	$CrCl_3.6H_2O$ (mol/L)	$NiCl_2.6H_2O$ (mol/L)	H_3BO_3 (mol/L)	$HCOONH_4$ (mol/L)	Glycine (mol/L)	NH_3 (25%) (g/L)	pH
Cr-1	0.4	---	0.7	1.8	1.0	124.6	7.0
Ni-1	---	0.2	0.7	1.8	1.0	124.6	7.0
(Ni-Cr)-1	0.4	0.2	0.7	1.8	1.0	124.6	7.0

In the presence of formate and glycine complexing agents, $[Cr(H_2O)_5Cl]^{+2}$ ions are converted to $[Cr(H_2O)_5(HCOO)]^{+2}$ and $[Cr(H_2O)_4(Gly)]^{+2}$. The formate complexes of Cr(III) are reduced through the following consecutive reaction steps to $Cr_{(s)}$:

$$[Cr(H_2O)_5(HCOO)]^{+2} + e^- \rightarrow [Cr(H_2O)_5(HCOO)]^{+} \quad (8)$$

$$[Cr(H_2O)_5(HCOO)]^{+} + 2e^- \rightarrow Cr_{(s)} + 5H_2O + HCOO^- \quad (9)$$

Similarly, the glycine complexes of Cr(III) are reduced through the following consecutive reaction steps to $Cr_{(s)}$:

$$[Cr(H_2O)_4(Gly)]^{+2} + e^- \rightarrow [Cr(H_2O)_4(Gly)]^{+} \quad (10)$$

$$[Cr(H_2O)_4(Gly)]^{+} + 2e^- \rightarrow Cr_{(s)} + 5H_2O + Gly^- \quad (11)$$

It is important to note that not all $[Cr(H_2O)_5(HCOO)]^{+2}$ and $[Cr(H_2O)_4(Gly)]^{+2}$ ions formed at the cathode are further reduced. Some of them are transported by electrolyte convection to the bulk solution. It is possible that a considerable amount of $[Cr(H_2O)_5(HCOO)]^{+}$ and $[Cr(H_2O)_4(Gly)]^{+}$ are decomposed to the stable $[Cr(H_2O)_5]^{+2}$.

Voltammetric behavior

Potentiodynamic cathodic polarization curves

Figure 1 shows the *i* vs. *E* curves for the deposition of chromium, nickel and Ni-Cr alloy codeposition under similar conditions. The curves were swept from the rest potentials to the more negative direction with scan rate of 20 mV/sec. Inspection of the data reveals that the Ni-Cr alloy deposited at a more noble potential than that of the individual deposition of Ni or Cr, indicating that chromium formed a solid solution with nickel.[15] Moreover, the polarization curve of the Ni-Cr alloy lies near to that of nickel deposit. Therefore, nickel-rich alloys are expected to deposit. The electrodeposition is characterized by high polarization as a result of formation of Cr(III) and/or Ni(II) complexes in the formate-glycine electrolytic bath. On the other hand, the curves of nickel and chromium exhibit a small limiting current plateau as a result of the limitation by diffusion processes. It should be noted that Ni-Cr codeposition is complicated by the simultaneous discharge of hydrogen ions, which occurs both during the separate electrodeposition of chromium and nickel. This is clear from the rapid increase in current in the polarization curve beyond the limiting current, especially for chromium deposition.

Increasing the concentration of either glycine (Fig. 2) or ammonium formate (Fig. 3) as complexing agents led to negative shifts of the polarization curves. This effect could be assigned to the increase in the stability of their corresponding complexes. On the other hand, increasing Cr(III) and Ni(II) ions in the bath (data are not included here), shifted the polarization curves towards the less negative potentials most probably due to an increase in the relative concentration of Cr(III) and Ni(II) ions, particularly in the diffusion layer.

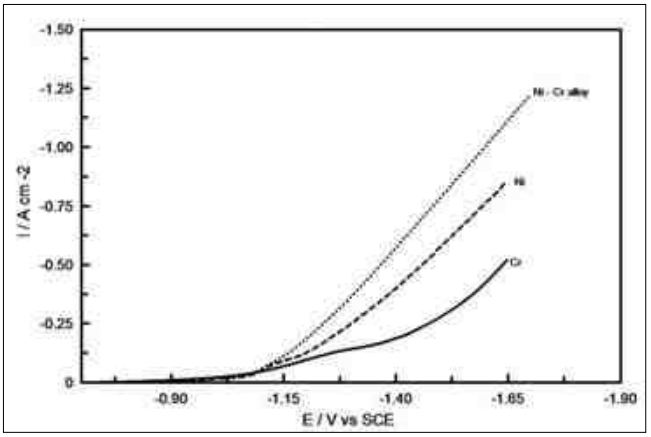

Figure 1—*Potentiodynamic cathodic polarization curves during the electrodeposition of chromium, nickel and Ni-Cr alloy from Baths Cr-1, Ni-1 and (Ni-Cr)-1, respectively.*

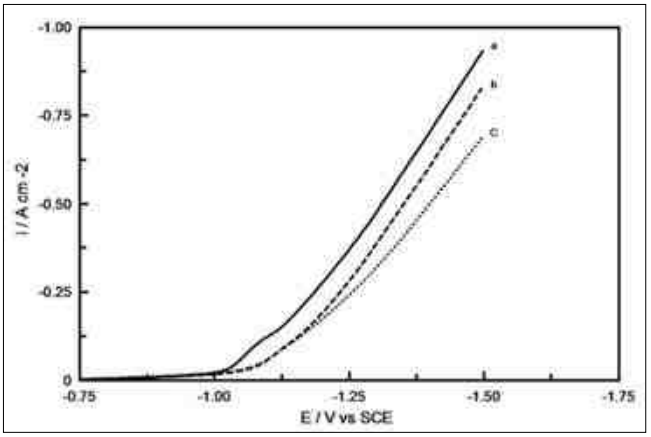

Figure 2—*Potentiodynamic cathodic polarization curves of Ni-Cr alloys codeposited from the (Ni-Cr)-1 bath but with different concentrations of glycine: (a) 0.3M, (b) 1.0M and (c) 1.5M.*

The influence of bath temperature on the cathodic polarization curves during Ni-Cr codeposition from the (Ni-Cr)-1 bath (Table 1) was examined and the results are shown in Fig. 4. The data reveals that a rise of bath temperature shifts the cathodic polarization curves to the less negative (more noble) values. This behavior could be related to the decrease in the activation overpotential of both hydrogen evolution[10,11] and Ni-Cr alloy codeposition reactions. Moreover, an increase of temperature enhances the concentration of the reducible species in the diffusion layer due to the increase in their diffusion coefficients. This effect is in addition to the effect of temperature on the relative abundance of both the complexed and uncomplexed species in the solutions.[8]

Cyclic voltammetry

Typical cyclic voltammetry recorded at the glassy carbon electrode (GCE) for chromium, nickel and Ni-Cr alloy from the Cr-1, Ni-1 and (Ni-Cr)-1 baths, respectively, is given in Fig. 5. The CV for chromium deposition showed a well defined cathodic peak at about -1.59 V during the cathodic scan and on reversing the scan in the anodic direction no anodic peaks were detected due to the high surface passivity. However, the CV for nickel deposition from a bath without Cr(III) ions, exhibited one small reduction peak at about -1.31 V and on reversing the scan in the positive direction, a small anodic peak at about -0.37 V with a peak current density of 1.4×10^{-4} A/cm^2 was detected as shown in Fig. 5. This small anodic peak is probably due to the nickel deposited on the substrate on the cathodic scan. The peak is very small due to the low concentration of Ni(II) in the Ni-1 bath. On the other hand, the CV recorded for Ni-Cr alloy codeposited from the (Ni-Cr)-1 bath exhibited a sharp and well defined reduction peak at about -1.28 V. This reduction peak lies at a more noble potential than that of the parent metals (Ni and Cr). These results are in good agreement with the results obtained by potentiodynamic polarization curves (Fig. 1). On reversing the scan in the positive direction, an anodic peak was detected at -0.33 V with peak current density of 4.2×10^{-4} A/cm^2. This anodic peak is probably due to the partial dissolution of nickel and Ni-Cr alloy simultaneously. In each case, a clear nucleation loop is observed in the forward scan which is typical for nucleation processes.

Some CVs were carried out at different scan rates (25 - 120 mV/sec) during Ni-Cr alloy codeposition and the relationship between the cathodic current peak i_{cp} and the square root of the scan rate $v^{1/2}$ (Fig. 6) was found to be linear, indicating diffusion control, *i.e.*, the rate of growth is controlled by mass transfer of Ni (II) and Cr(III) ions to the growing center. However, the negative value of the cathodic peak current density i_{cp} at $v^{1/2} = 0$, is consistent with a deposition process involving a nucleation mechanism controlled by mass transfer.[8]

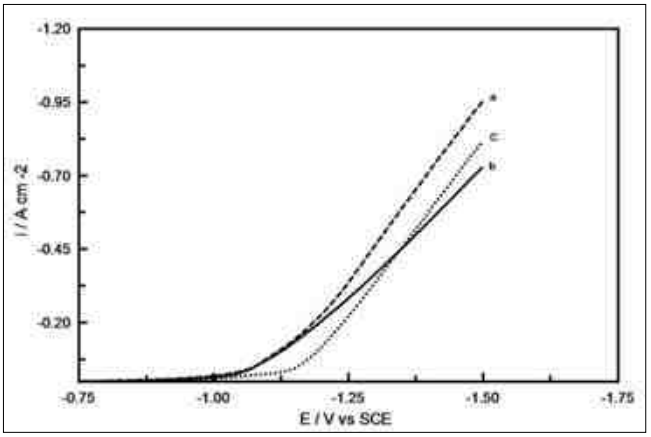

Figure 3—*Potentiodynamic cathodic polarization curves of Ni-Cr alloys codeposited from the (Ni-Cr)-1 bath but with different concentrations of ammonium formate: (a) 1.0M, (b) 1.2M and (c) 1.5M.*

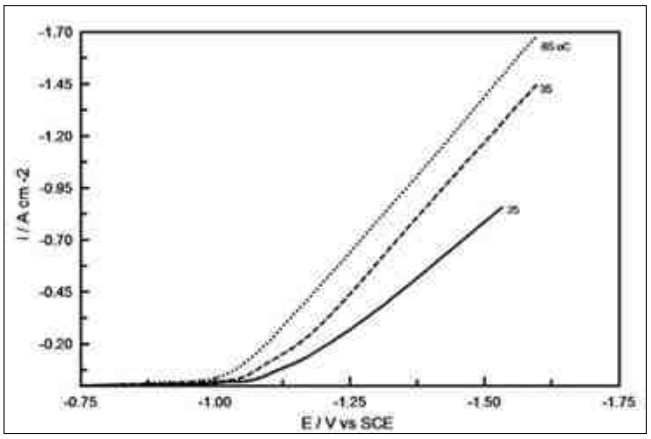

Figure 4—*Potentiodynamic cathodic polarization curves of Ni-Cr alloys codeposited from the (Ni-Cr)-1 bath at different temperatures.*

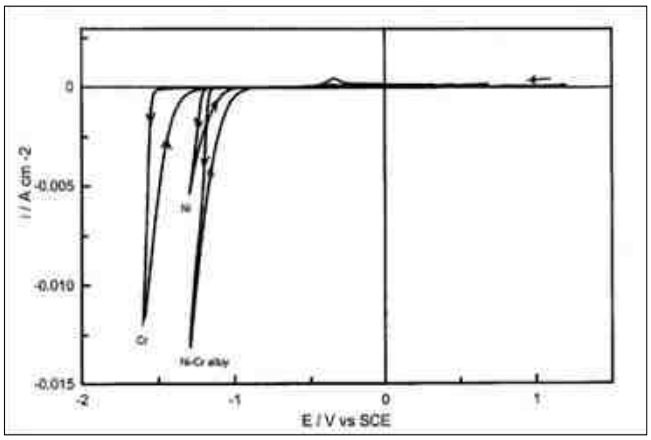

Figure 5—*Cyclic voltammetry recorded at the glassy carbon electrode for chromium electrodeposition, nickel electrodeposition and Ni-Cr alloy at a scan rate of 50 mV/sec.*

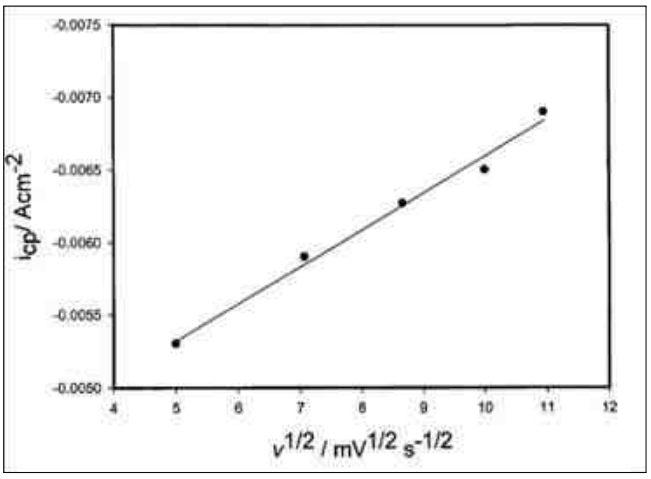

Figure 6—*Plot of cathodic peak current (i_{cp}) vs. the square root of the scan rate $v^{1/2}$ for Ni-Cr alloy codeposition.*

Cathodic current efficiency and composition of Ni-Cr alloys

In most cases studied the cathodic current efficiency (CCE) of Ni-Cr alloys codeposited from formate-glycine baths is less than 100%, denoting simultaneous hydrogen evolution. The effect of bath composition, and some plating parameters on the overall CCE of the alloy deposition as well as on chromium content in the deposits were analyzed and the results are given in Figs. 7-12.

The effect of applied deposition current density (from 0.33 to 11.7 A/dm^2) on the chromium content in the alloy as well as on the overall CCE of the alloy is given in Fig. 7. At very low current density, the CCE is relatively high (40%), probably due to the low rate of hydrogen evolution. Further increase in current density decreases the CCE, which then tends to level off at about 25%. On the other hand, increasing current density increases the at% chromium to a maximum value of 25.1% at a current density of 0.67 A/dm^2, and then with further increase in current density, the at% chromium decreases to 1.5% at 11.7 A/dm^2. For this reason, a current density of 0.67 A/dm^2 was chosen for further experiments when using fixed constant current. This decrease in at% chromium is probably due to the significant hydrogen evolution with increasing current density. The decrease of chromium content with current density is in good agreement with results reported during the pulse plating of Ni-Cr alloy.[20]

Figure 8 shows the effect of increasing Ni(II) ions in the bath on the at% chromium and on CCE%. Increasing Ni(II) ions slightly decreases the chromium content and then increases it again with a further increase in Ni(II) ions. The effect is the reverse with the CCE.

Figure 9 depicts the influence of increasing Cr(III) ions content in the bath (0.6 to 1.0M) on the CCE of the alloy deposition as well as on the at% chromium in the deposit. It is clear that increasing the Cr(III) ion concentration has a significant effect on the deposition process. This means that increasing the Cr(III) ion concentration improves the chromium deposition rate.[18] On the other hand, increasing Cr(III) in the bath greatly decreases the current efficiency of the alloy deposition.

An increase in bath temperature from 25 to 60°C has a pronounced increasing effect on the CCE of the alloy deposition (Fig. 10) and a decreasing effect on the chromium content in the alloy. The increase in CCE with bath temperature is consistent with the

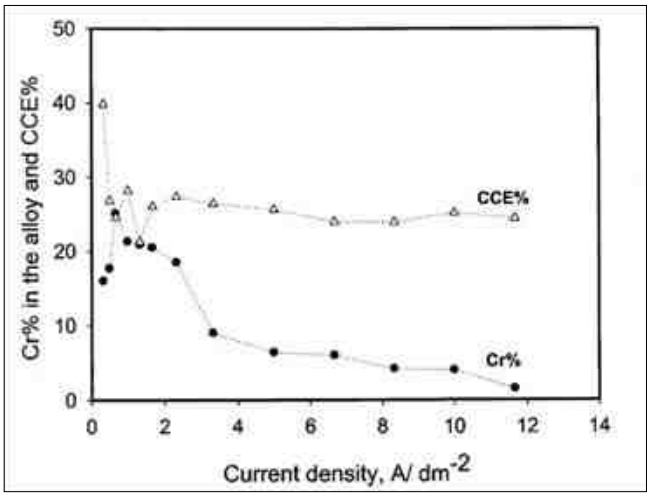

Figure 7—*Effect of the applied deposition current density on at% chromium and on the CCE during the codeposition of Ni-Cr alloy from the selected bath.*

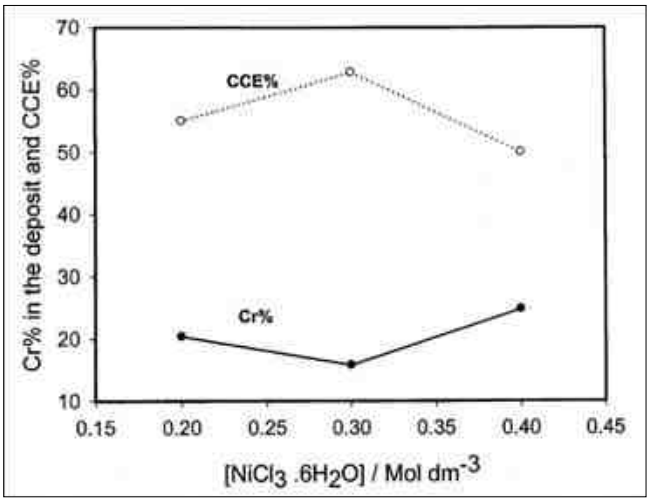

Figure 8—*Effect of $NiCl_2{\cdot}6H_2O$ concentration on at% chromium and on the CCE during the codeposition of Ni-Cr alloy from the (Ni-Cr)-1 bath; i = 0.67 A/dm^2.*

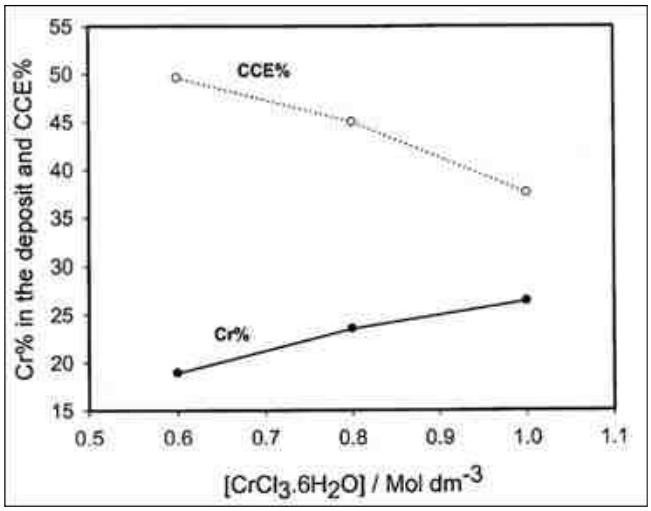

Figure 9—*Effect of $CrCl_3{\cdot}6H_2O$ concentration on at% chromium and on the CCE during the codeposition of Ni-Cr alloy from the (Ni-Cr)-1 bath, i = 0.67 A/dm^2.*

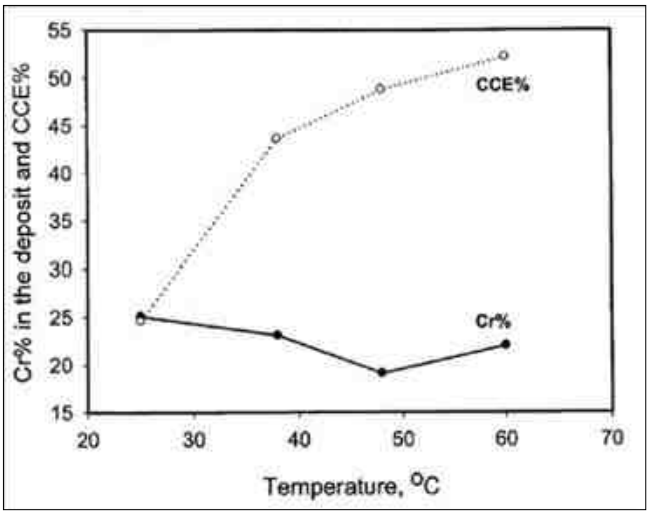

Figure 10—*Effect of temperature on at% chromium and on the CCE during the codeposition of Ni-Cr alloy from the (Ni-Cr)-1 bath, i = 0.67 A/dm^2.*

results of the polarization curves shown in Fig. 4. It is worthwhile to mention here that the ambient temperature has a significant advantage in practical operations for producing alloys of high chromium content from this complex bath, but the disadvantage is the low CCE.

An increase in the glycine concentration from 0.5 to 2.0M slightly increased the chromium content but decreased the CCE of the alloy codeposition (Fig. 11). This means that glycine accelerates the chromium deposition in the alloy although it has an increasing effect on the polarization curves (Fig. 2).

On the other hand, an increase in the ammonium formate concentration from 1.0 to 1.8M decreased the chromium content to a minimum value and then it increased again with a further increase in ammonium formate concentration (Fig. 12). However, the CCE increased to a maximum value and then decreased slightly with a further increase in the ammonium formate concentration.

Inspection of the data in Figs. 10-12 showed that any parameters which increased the chromium content in the deposit led to a decrease in the CCE of the alloy deposition. This result could likely be attributed to the fact that chromium deposition is accompanied by simultaneous hydrogen evolution, which leads to such a decrease.

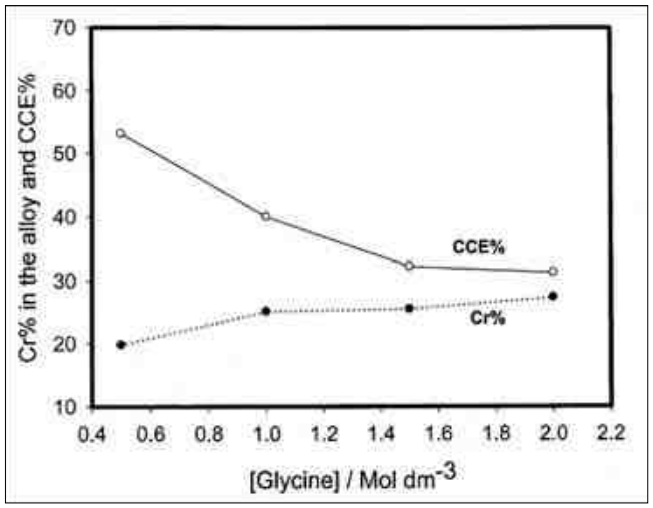

Figure 11—*Effect of glycine concentrations on at% chromium and on the CCE during the codeposition of Ni-Cr alloy from the (Ni-Cr)-1 bath, i = 0.67 A/dm².*

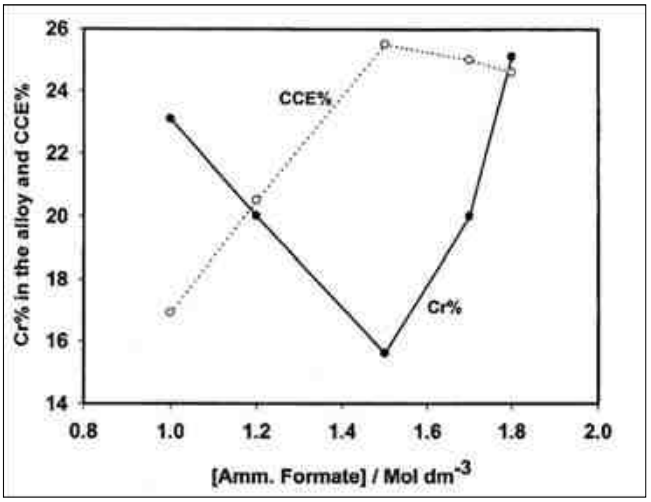

Figure 12—*Effect of ammonium formate concentrations on at% chromium and on the CCE during the codeposition of Ni-Cr alloy from the (Ni-Cr)-1 bath, i = 0.67 A/dm².*

Chronoamperometric measurements

Potentiostatic current-time transients, when used for studying the kinetics of nucleation and growth of nuclei of a metallic phase, have some advantages over cyclic voltammetry. The nucleation occurs at constant cathodic potential, determining constant values of the nucleation work and the charge transfer rate for the entire surface of an energy-uniform electrode within a specified time period. For this purpose, a series of current-time transients at a given deposition potential, for Ni-Cr codeposition from the formate-glycine bath, was measured and some representative data are given in Fig. 13. The transient current decreased monotonically with time to reach a steady-state value. The decrease in current in the initial stages of the transient is related to double-layer charging.[21] As the cathodic step potential is made more negative, the values of the instantaneous and steady-state current increase. Plotting of the current density i versus $t^{-1/2}$ according to the Cotrell equation[22] for the descending parts of the current transients shows straight lines with an R^2 value of 0.998. This very high value for the correlation confirms that the growth of the Ni-Cr alloy is a diffusion-controlled process (Fig. 13 inset). The slopes of the lines depend on the values of the step potentials.

Morphology of the Ni-Cr thin films

Figure 14 shows the SEM images of the as-deposited Ni-Cr alloys from the Cr(III) glycine-formate complex bath at different applied deposition current densities. As can be observed, at very low current densities (0.3 and 0.5 A/dm²), the surface of the deposit is milky, crack-free and consists of non-uniform multilayers (Figs. 14a,b). However, further increase in the current density (≥ 0.7 A/dm²) leads to formation of shallow cracks on the surface (Figs. 14c,d). The crack formation is well known and characteristic of chromium and chromium alloy deposits.[23,24] The appearance of cracks at higher current densities can be explained by internal stress developed during film formation in response to the evolution of hydrogen gas. It is generally believed that surface cracking in a chromium deposit could reduce the residual stress developed during the electrodeposition of chromium and chromium alloys.[25] On the other hand, the addition of a high glycine concentration in the bath increases the network of cracks on the surface, as seen in Fig. 14e. It is worthwhile to mention here that increasing glycine concentration increases the chromium content in the alloy deposit (Fig. 11).

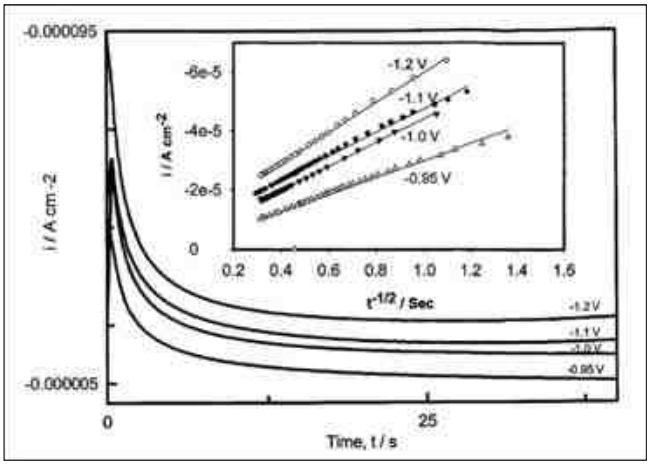

Figure 13—*Chronoamperometric current-time transients for Ni-Cr alloy codeposition from (Ni-Cr)-1 bath at different deposition potentials; inside is the relationship between the transient current i and the $t^{-1/2}$ at different deposition potentials.*

Microstructure of Ni-Cr coatings

It has been well known that the physical properties of codeposited Ni-Cr films depend on their structural characteristics. Therefore, it is very important to investigate the crystallographic structures of the electrodeposited thin films.[26] A series of experiments were carried out to find the effect of current density on the microstructure of Ni-Cr deposits (Fig. 15). The appearance of broad peaks at $2\theta = 52°$ and at $2\theta = 77°$ indicates that the Ni-Cr alloy structure is amorphous at all current densities. The increase in the amorphous nature of the alloy can be assumed to enhance the corrosion resistance of the materials.[27] It is known that amorphous electrodeposited alloys, which contain passivating elements such as chromium, have higher corrosion resistance compared with microcrystalline and crystalline samples with the same composition.[28]

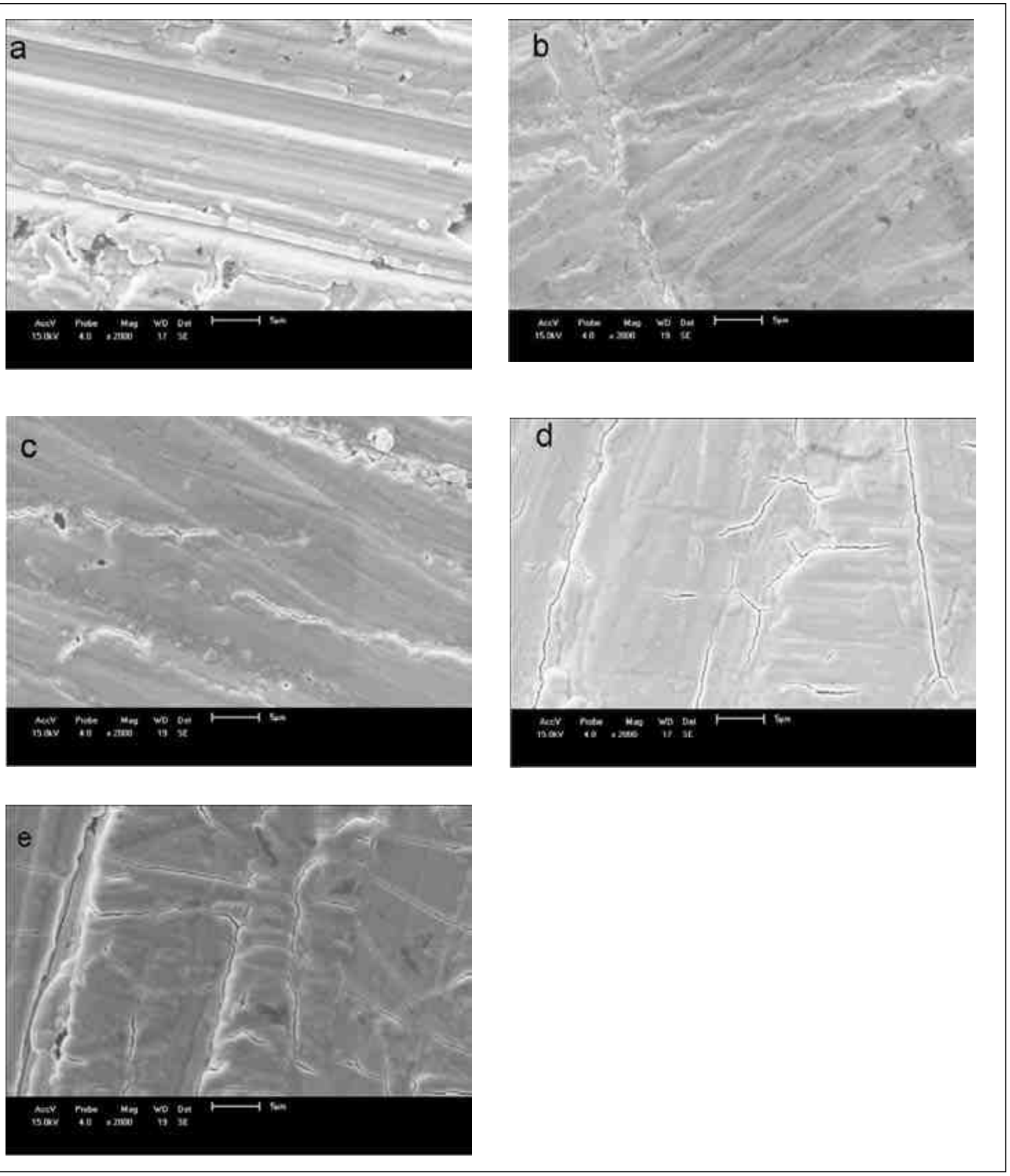

Figure 14—*Photomicrographs of Ni-Cr alloy codeposited from (Ni-Cr)-1 bath at: a) 0.3 A/dm², b) 0.5 A/dm², c) 0.7 A/dm², d) 1.0 A/dm² and (e) same as c) but with an excess concentration of glycine (1.5M).*

Corrosion behavior

The performance of any coating of a thin film for industrial application is tested for its stability, *i.e.*, corrosion resistance under natural environmental conditions.[29] Figure 16 illustrates characteristic anodic potentiodynamic curves of nickel and Ni-Cr alloy. The investigation was carried out in 0.1M NaOH solution. The curves were obtained by sweeping the potential starting from -1.4 V_{SCE} where hydrogen evolution was dominant, up to an anodic potential of 0 V_{SCE} at a scan rate of 10 mV/sec. The measurements were also performed for uncoated steel for comparison. As can be seen, the nickel-coated steel and the uncoated steel exhibited an active-passive-transpassive behavior. The Ni-Cr thin film deposited from formate-glycine electrolyte, on the other hand, does not exhibit a region of active anodic dissolution. The passive region is characterized by the wide range of passivity (about 0.5 V), as well as a low anodic current density (2.7×10^{-4} A/cm^2).

The uncoated steel is dissolved, being in active anodic state with a high corrosion rate, and its maximum is reached at 3.5×10^{-3} A/cm^2. This means that with Ni-Cr deposited on steel, a typical passive state is reached and the values of the anodic current remain low within a large potential range. On the other hand, although the corrosion potential E_{corr} for the Ni-Cr alloy is close to that of uncoated steel, the i_{corr} for the Ni-Cr alloy (1.73×10^{-5} A/cm^2) is less than that of uncoated steel (2.4×10^{-5} A/cm^2). This means that the Ni-Cr thin film will protect steel from corrosion.

Conclusions

The following conclusions can be drawn from this study:

1. The codeposition of highly adherent thin film of Ni-Cr alloys onto steel substrates from a complexing Cr(III) formate-glycine baths was successfully achieved containing up to 28 at% chromium depending on the operating conditions.
2. The chromium content in the alloy increased with increasing in Ni^{+2} ion content as well as with Cr^{+3} ion content. However, the chromium content decreased with increasing temperature.
3. Increasing the current density increased the chromium content to a maximum value of 25.1 at% at a current density of 0.67 A/dm^2 and then with further increase in current, the chromium content decreased to 1.5 at% at 11.7 A/dm^2.
4. An increase in bath temperature has a pronounced increasing effect on the cathode current efficiency of the alloy deposition and a decreasing effect on the chromium content in the alloy.
5. Cyclic voltammetry and potentiodynamic polarization measurements showed that the Ni-Cr deposition potential lies at a more noble potential than that of the parent metals, indicating that chromium forms a solid solution with nickel.
6. The chronoamperometric measurements indicated that the initial growth of Ni-Cr alloy codeposition is a diffusion-controlled process, while, the XRD measurements showed that all Ni-Cr alloy deposits were amorphous.

Acknowledgments

The authors gratefully acknowledge Taibah University for their financial support.

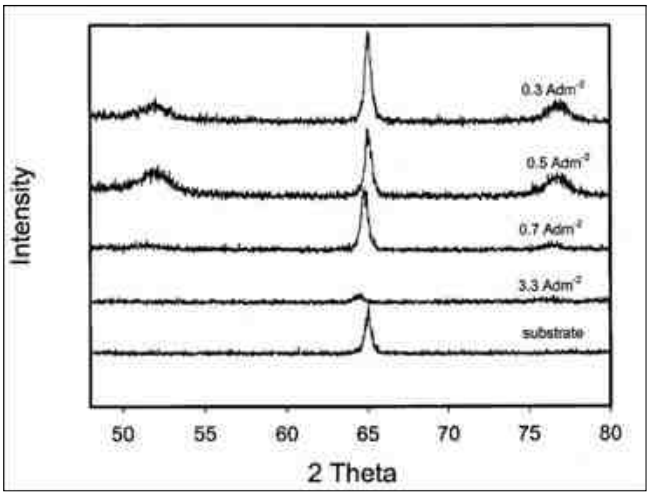

Figure 15—*XRD analysis of the as-deposited Ni-Cr alloy at different applied deposition current densities.*

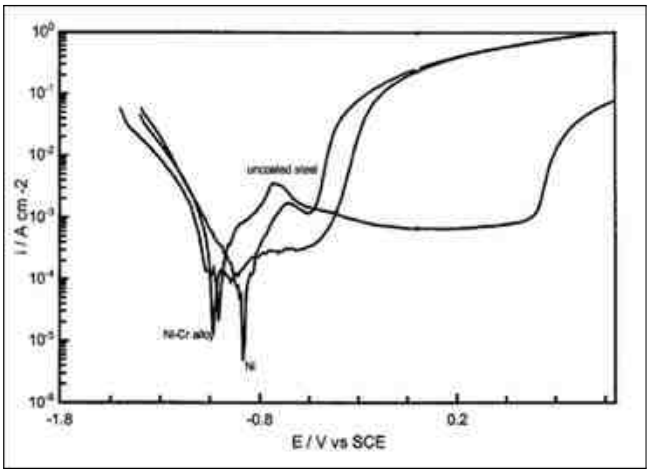

Figure 16—*Potentiodynamic anodic curves for the as-deposited Ni-Cr alloy, nickel and for uncoated steel in 0.1M NaOH solution.*

References

1. G.B. Hoflund & W.S. Epling, *Thin Solid Films*, **307** (1-2), 126 (1997).
2. J.K. Dennis & T.E. Such, *Nickel and Chromium Plating*, Butterworth, London, UK, 1972; p. 186.
3. D.L. Duan, *et al.*, *Mat. Sci. and Technol.*, **24** (4), 461 (2008).
4. H-Y. Lin, *et al.*, *Dental Materials*, **24** (3), 378 (2008).
5. S. Survilienė, *et al.*, *Applied Surface Science*, **253** (16), 6738 (2007).
6. B. Li, *et al.*, *J. Alloys and Compounds*, **453** (1-2), 93 (2008).
7. J. McDougall, M. El-Sharif & S. Ma, *J. Appl. Electrochem.*, **28** (9), 929 (1998).
8. S.S. Abd El Rehim, *et al.*, *Trans. Inst. Met. Finish.*, **80** (1), 29 (2002).
9. M.A.M. Ibrahim, *J. Appl. Surf. Finish.*, **3** (2), 89 (2008).
10. M.A.M. Ibrahim *et al.*, *Plating & Surface Finishing*, **86** (4), 69 (1999).
11. S.S. Abd El Rehim, *et al.*, *J. Chem. Technol. Biotechnol.*, **73** (4), 369 (1998)
12. S.S. Abd El Rehim, *et al.*, *Trans. Inst. Met. Finish.*, **80** (3), 105 (2002).
13. S.S. Abd El Rehim, M.A.M. Ibrahim & M.M. Dankeria, *J. Appl. Electrochem.*, **32** (9), 1019 (2002).
14. M.A.M. Ibrahim, S.S. Abd El Rehim & S.O. Moussa, *et al.*, *J. Appl. Electrochem.*, **33** (7), 627 (2003).
15. A. Brenner, *Electrodeposition of Alloys: Principles and Practice - Vol. 2*, Academic Press, New York, NY, 1963.
16. J-Y. Hwang, *Plating & Surface Finishing*, **78** (5), 118 (1991).

17. A.A. Edigaryan & Y.M. Polukarov, *Russian J. Appl. Chem.*, **76** (2), 323 (2003).
18. Y.M. Polukarov, *et al.*, *Protection of Metals*, **37** (5), 447 (2001).
19. S.K. Ibrahim, *et al.*, *Trans. Inst. Met. Finish.*, **76** (4), 156 (1998).
20. C.A. Huang, *et al.*, *Scripta Materialia*, **57** (1), 61 (2007).
21. G. Trejo, A.F. Gil & I. González, *J. Appl. Electrochem.*, **26** (12), 1287 (1996).
22. F.J. Barry & V.J. Cunnane, *J. Electroanal. Chem.*, **537** (1-2), 151 (2002).
23. B. Li, A. Lin & F. Gan, *Surf. & Coat. Technol.*, **201** (6), 2578 (2006).
24. S.C. Kwon, *et al.*, *Surf. & Coat. Technol.*, **183** (2-3), 151 (2004).
25. C.A. Huang, W. Lin & M.J. Liao, *Corrosion Science*, **48** (2), 460 (2006).
26. J.P. Branciaroli (J.H. Lindsay, Ed.), *Plating & Surface Finishing*, **88** (10), 12 (2001).
27. M.A.M. Ibrahim, S.F. Korablov & M. Yoshimura, *Corrosion Science*, **44** (4), 815 (2002).
28. C.A.C. Souzaa, *et al.*, *Surf. & Coat. Technol.*, **190** (1), 75 (2005).
29. C.N. Tharamani, *et al.*, *J. Electrochem. Soc.*, **153** (3), C164 (2006).

About the authors

Dr. Magdy A.M. Ibrahim *is Associate Professor of Electrochemistry in the Chemistry Department, Faculty of Science, Ain Shams University in Cairo, Egypt. He holds M.Sc. and Ph.D. degrees in Electrochemistry from Ain Shams University. He held a scholarship in Germany at Erlangen-Nuremberg University (1992-1994). He was a UNESCO fellow for the 35th International Course for Advanced Chemistry and Chemical Engineering at the Tokyo Institute of Technology from (1999-2000) and was a visiting researcher there as well (2000-2001). Since 2003, he has been working as an Associate Professor at Taibah University in Saudi Arabia. His research interests include electroplating of metals and alloys, and corrosion of metals.*

Dr. S.N. Alamri *is Associate Professor of Applied Physics in the Physics Department, Faculty of Science, Taibah University in Saudi Arabia. He holds a Ph.D. degree in thin film CdS/CdTe Solar Cells from Durham University, England (1999). His research interests are in thin film deposition and characterization.*

Dr. M. Emad *is a Lecturer of Chemistry at Chemistry Department, Faculty of Science, Taibah University in Saudi Arabia. He holds a Ph.D. degree from Ain Shams University, Egypt (1999). His research interests are in the field of corrosion inhibition and water analysis.*